

CHAPTER 7**X-RAY DIFFRACTION AND SCANNING ELECTRON MICROSCOPY
ANALYSIS OF CHITOSAN COMPLEXES AND COMPOSITES****7.1 Introduction**

X-ray diffraction can shed some light on the degree of crystallinity/amorphousness of a sample. In turn these parameters can help explain conductivity variation among materials comprising the same components, but different compositions. Morphology studies can complement results from x-ray studies. Morphology studies in chitosan complexes have been performed using SEM.

7.2 X-ray diffraction of chitosan-NH₄SCN

Fig. 7.1 depicts the XRD pattern of chitosan - NH₄SCN complexes with varying salt concentrations. From Fig. 7.1, peaks at $2\theta = 15^\circ$ and 21.6° was observed for pure chitosan. With 10 wt.% of NH₄SCN introduced into chitosan, the intensity of the peak at $2\theta = 15^\circ$ decreased and have become broader indicating the sample is more amorphous compared to pure chitosan. This also shows that complexation between chitosan and NH₄SCN has occurred. NH₄SCN has helped in reducing the degree of crystallinity of chitosan. With 20 wt.% NH₄SCN added, the XRD pattern has become broader than that of 10 wt.% NH₄SCN sample with peak at $2\theta = 15^\circ$ split into three small peaks at $2\theta = 11.6^\circ$, 15.4° and 19.1° .

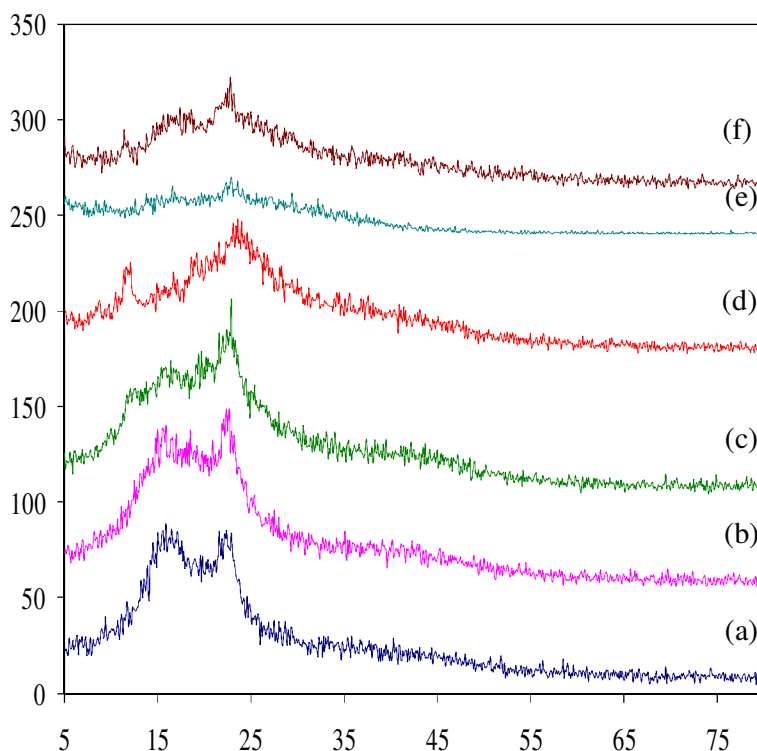


Fig. 7.1: XRD patterns of chitosan with (a) 0 wt.% (b) 10 wt.% (c) 20 wt.% (d) 30 wt.% (e) 40 wt.% (f) 50 wt% NH_4SCN concentration.

Peak at $2\theta = 22.6^\circ$ was found to become broader in sample containing 30 wt.% NH_4SCN and has shifted from $2\theta = 21.6^\circ$ in 20 wt.% NH_4SCN sample to 22.6° . This is attributed to complexation between chitosan and NH_4SCN salt. With 40 wt.% NH_4SCN added, XRD pattern is most amorphous compared to others. It is well known that, as amorphousness increased, the conductivity will increase too. From impedance studies, it has been proven that conductivity for sample containing 40 wt.% NH_4SCN has the highest conductivity value at room temperature. With addition of 50 wt.% NH_4SCN the crystallinity of the sample increased again. Crystalline peaks at $2\theta = 11.2^\circ$, 15.6° and 22.3° are observed. From this study it is also understood that the increase in conductivity is not only due to the increase in number density of mobile ions but also due to the increase in amorphousness of the material. It is also understood that the

decrease in conductivity with more than 40 wt.% salt added is due to decrease in amorphousness of the material.

7.3 Surface Morphology of Chitosan- Al_2TiO_5 Composite Film

Fig. 7.2 shows the SEM micrograph of pure chitosan acetate. The surface is smooth and homogeneous. The XRD pattern of chitosan acetate is shown in the inset with peaks at $2\theta = 15^\circ$ and 21.6° .

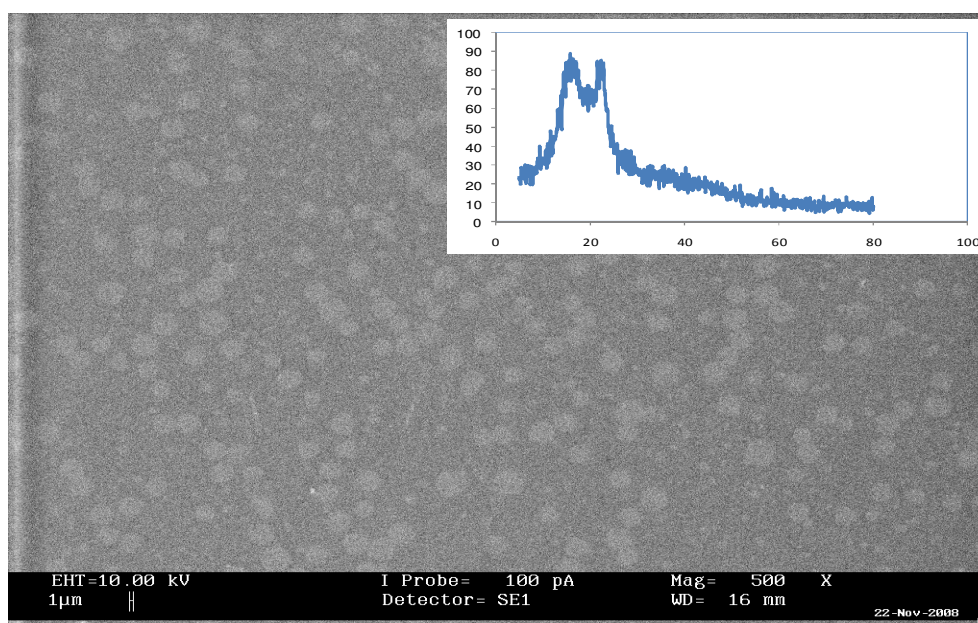
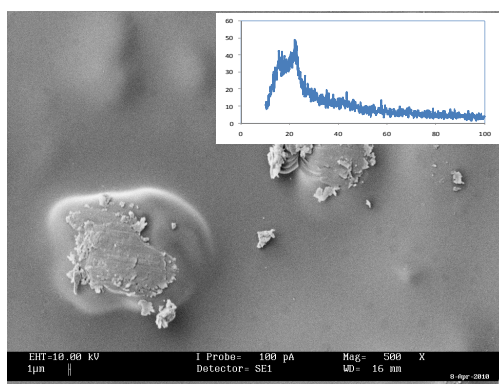
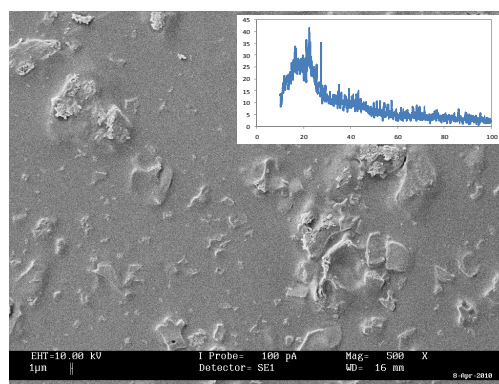


Fig. 7.2: SEM surface morphology of chitosan acetate film

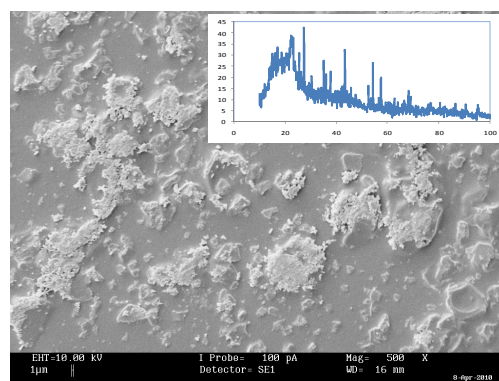
XRD diffractogram and SEM micrograph of the surface morphology of chitosan- Al_2TiO_5 film with various compositions of Al_2TiO_5 are shown in Fig. 7.3 (a) until (j).



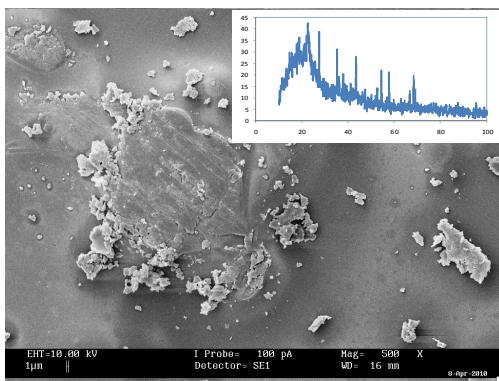
(a)



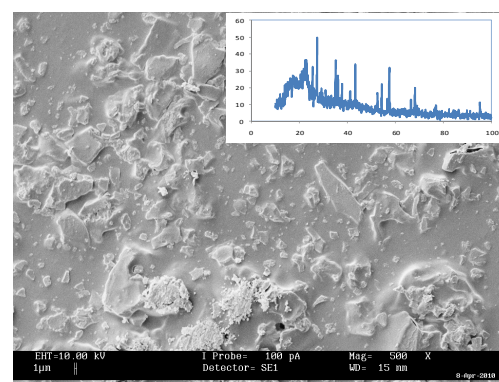
(b)



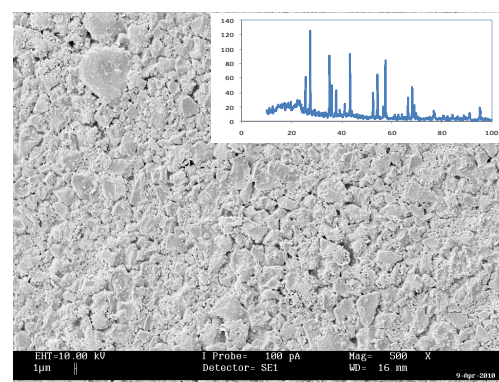
(c)



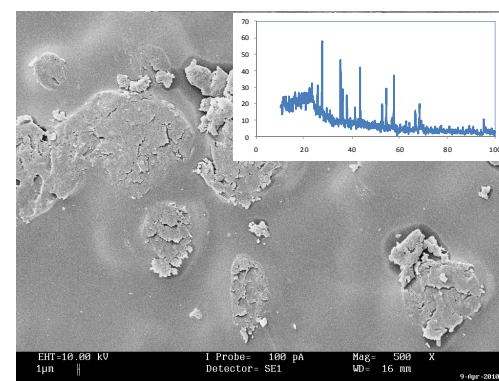
(d)



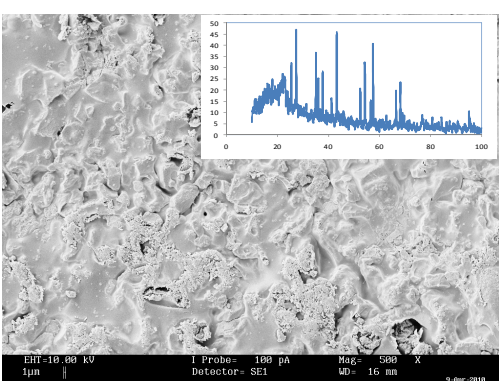
(e)



(f)



(g)



(h)

Fig. 7.3 continued.....

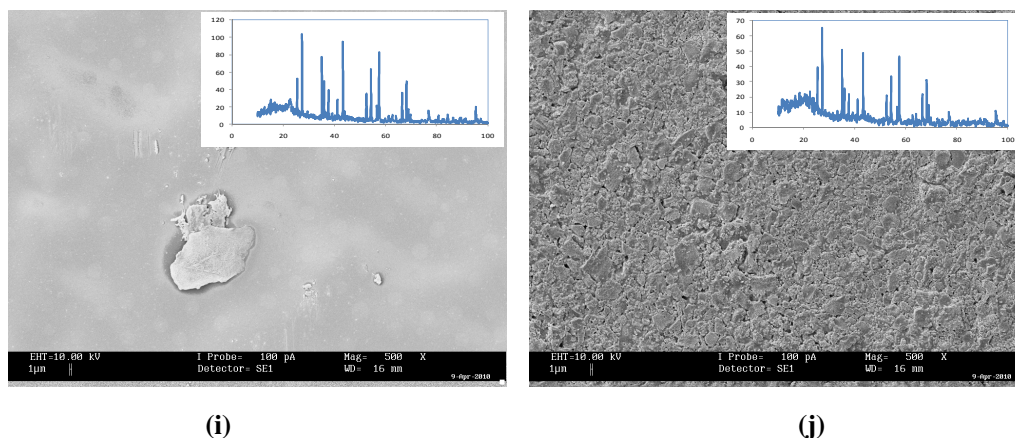


Fig. 7.3: SEM surface morphology of chitosan with (a) 5 wt.% (b) 10 wt.% (c) 15 wt.% (d) 20 wt.% (e) 25 wt.% (f) 30 wt.% (g) 35 wt.% (h) 40 wt.% (i) 45 wt.% and (j) 50 wt.% Al_2TiO_5 film

Upon addition of 5 wt.% Al_2TiO_5 , the SEM micrograph shows that the smooth surface of chitosan-acetate film has become rough. Some agglomerates can be observed on the surface of the composite film. These agglomerates could be due to Al_2TiO_5 from peaks at $2\theta = 42.4^\circ$ and 56.5° in the x-ray diffractogram. The average size of agglomerates is around $668 \mu\text{m}^2$. Peaks at $2\theta = 15^\circ$ and 21.6° due to chitosan is observed to be broader.

On addition of 10 wt.% Al_2TiO_5 , the surface becomes rougher with more agglomerates, but with smaller size, compared to those in Fig. 7.3(a). A peak at $2\theta = 27.5^\circ$ corresponding to Al_2TiO_5 is observed. Smaller peaks due to Al_2TiO_5 are also observed at $2\theta = 26.1^\circ$ and 56.5° . Peaks due to chitosan decreased in intensity. Coherent length calculated for the peak at $2\theta = 27.5^\circ$ is 68 nm.

As 15 wt.% of Al_2TiO_5 was added, the agglomeration due to Al_2TiO_5 is bigger and larger compared to sample containing 10 wt.% Al_2TiO_5 . Peaks that correspond to Al_2TiO_5 are more obvious. Meanwhile peaks of chitosan has become broader and

decreased in intensity compared to that of pure chitosan. Coherent length for this sample calculated from peak at 27.5° has increased to 89 nm. The agglomeration has increased and the average size is around $10217 \mu\text{m}^2$ for sample containing 20 wt.% Al_2TiO_5 . The structure is more crystalline compared to pure chitosan with coherent length of 63 nm. As more Al_2TiO_5 added (30 wt.% Al_2TiO_5), the surface roughness increased. Agglomeration increased and is more packed. Peaks due to Al_2TiO_5 are observed to be distinct while chitosan peaks continuing to decrease in intensity. Coherent length for this sample is increase to 110 nm.

With 35 wt.% Al_2TiO_5 added, the agglomeration average size is found to be around $624 \mu\text{m}^2$. Coherent length is 104 nm. Al_2TiO_5 peaks are more distinct and chitosan peaks decreased in intensity. As more Al_2TiO_5 added, the surface roughness increased and become fully packed with agglomerates. The condition of agglomeration on the surface is varied due to uneven distribution of Al_2TiO_5 in the chitosan acetate matrix. As Al_2TiO_5 content increased up to 50 wt.%, the XRD shows peaks of Al_2TiO_5 and its intensity increased. Peaks can be observed at $2\theta = 25.6^\circ, 27.5^\circ, 35.15^\circ, 43.4^\circ, 57.55^\circ$ and 66.5° due to Al_2TiO_5 . Coherent length for sample containing 50 wt.% Al_2TiO_5 is 125 nm. It can therefore be inferred that the Al_2TiO_5 increases the roughness of the chitosan acetate surface. XRD shows that some parts of the sample maintained its amorphousness from the broadness of the peak and some parts have become more crystalline.

7.4 SEM Micrograph of Chitosan - NH_4SCN Film

SEM micrograph of chitosan acetate film containing 40 wt.% NH_4SCN is shown in Fig. 7.4. The surface appears uneven but smooth. The XRD pattern showed that pure

chitosan (Fig. 7.2) has become more amorphous when 40 wt.% NH_4SCN was added into the polymer. This also indicates that complexation between chitosan and NH_4SCN has occurred.

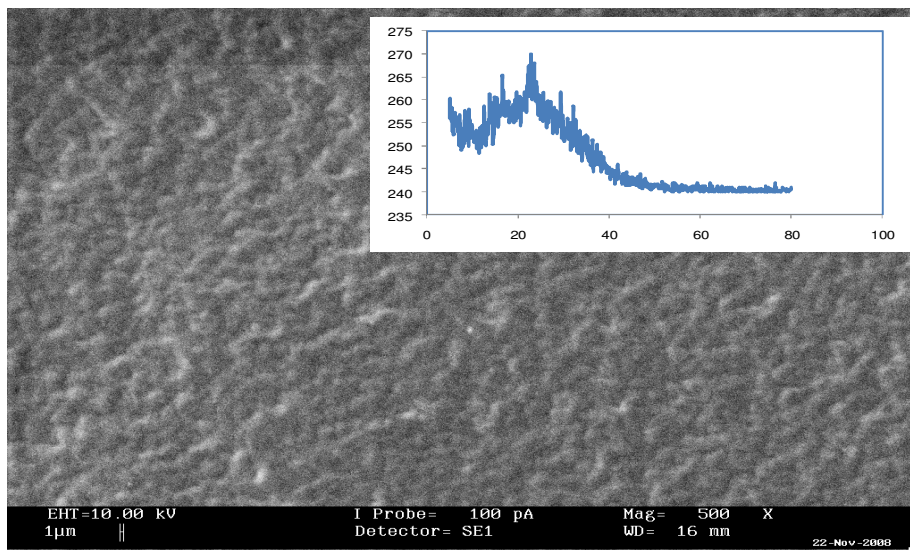
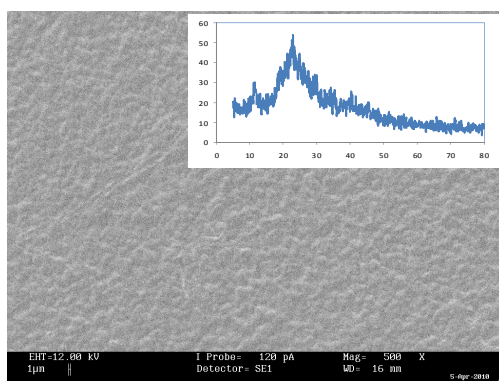


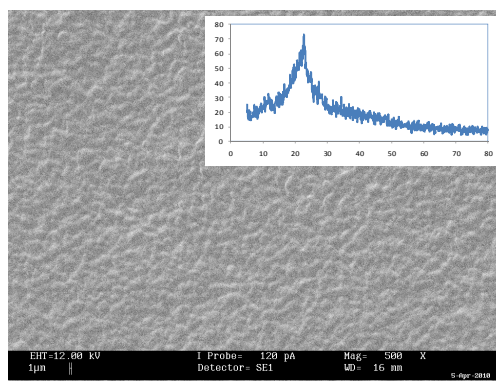
Fig. 7.4: SEM surface morphology of chitosan - NH_4SCN film

7.5 SEM Micrographs of (Chitosan – NH_4SCN) + Al_2TiO_5 Film

The effect of adding Al_2TiO_5 on the morphology of the highest conducting sample of 60 wt.% chitosan-40 wt.% NH_4SCN is shown in Fig. 7.5 (a) until (e). It can be seen that with the addition of salt, the surface morphology become more amorphous compared to chitosan- Al_2TiO_5 samples in Fig. 7.3.



(a)



(b)

Fig. 7.5 continued.....

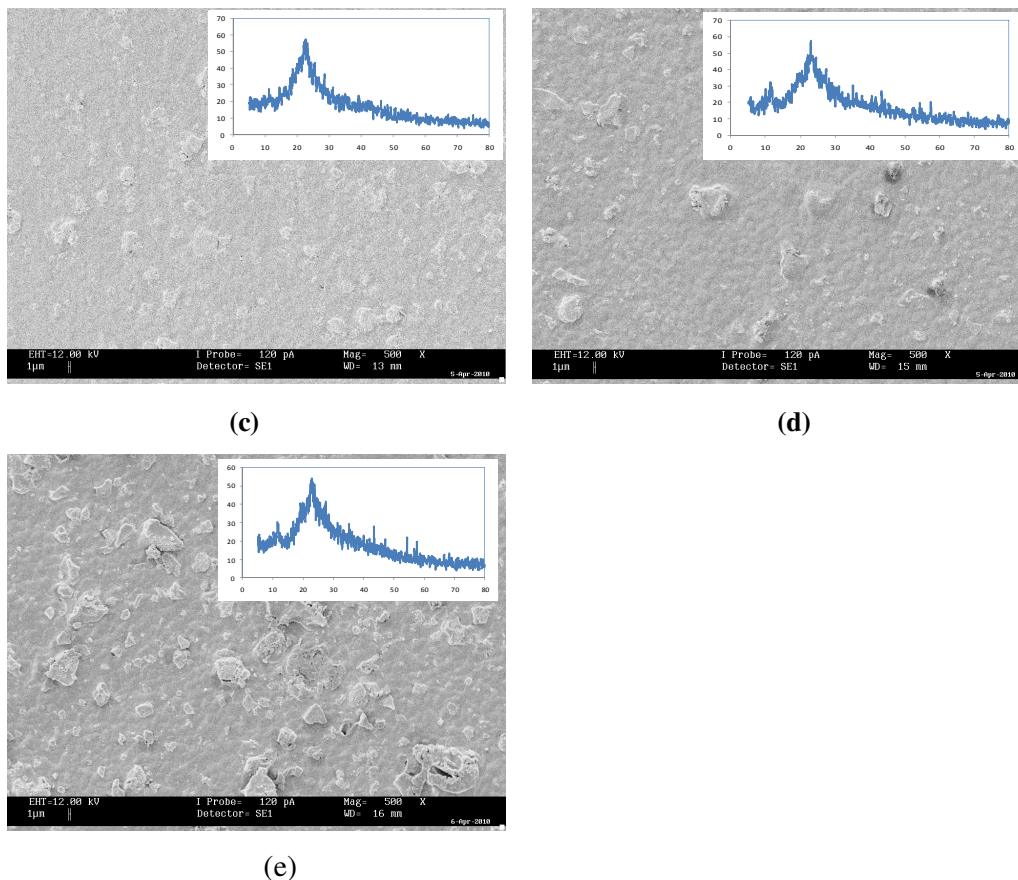


Fig. 7.5: SEM surface morphology of chitosan-NH₄SCN with (a) 1 wt.% (b) 2 wt.% (c) 4 wt.% (d) 5 wt.% and (e) 7 wt.% Al₂TiO₅.

With addition of Al₂TiO₅ into the chitosan-NH₄SCN film, the peak at $2\theta = 22.1^\circ$ narrowed and appears sharper compared to Fig. 7.4. This shows that the sample has become more crystalline. This supports the decrease in conductivity on addition of 1 wt.% Al₂TiO₅. On addition of 4 wt.% Al₂TiO₅, additional peaks are observed at $2\theta = 26.8^\circ, 29.3^\circ, 39.1^\circ$ and 46.3° and the conductivity is even lower than that of the chitosan-NH₄SCN complex with 1 wt.% and 2 wt.% Al₂TiO₅. Although the surface morphology did not show much change, the XRD results support the results of conductivity versus Al₂TiO₅ as depicted in Chapter 5, up to 4 wt.% Al₂TiO₅.

With addition of 5 wt.% Al_2TiO_5 , the agglomerates are more distinct. The surface roughness increased. More peaks are observed at $2\theta = 11.3^\circ, 25.5^\circ, 35.1^\circ, 43.3^\circ, 54.3^\circ$ and 57.5° . This indicates the sample is semi-amorphous. Even though more agglomerates exist in this sample compared to sample with 4 wt.% Al_2TiO_5 , this sample exhibits the highest conductivity. This might be due to the existence of hydroxides or OH functional groups on the surface of Al_2TiO_5 . This hydroxide groups help to provide additional pathways for ions to hop easily with lower activation energy thus, increasing the conductivity. After addition of 7 wt.% Al_2TiO_5 , more agglomerates and some parts on the surface of the sample appear torn. Peaks are observed at $2\theta = 25.5^\circ, 35.1^\circ, 43.3^\circ, 54.3^\circ$ and 57.5° are sharper than those in sample containing 5 wt.% Al_2TiO_5 . This shows that the sample has become more crystalline, which supports the decrease in conductivity. Fig. 7.6 shows the conductivity and coherent length with variation of Al_2TiO_5 (wt.%). Coherent length was calculated for peak at $2\theta = 22.3^\circ$. Coherent length is inversely proportional to conductivity. The smallest coherent length is in sample containing 5 wt.% Al_2TiO_5 is 3.33 nm. This results support the conductivity is highest at 5 wt.% Al_2TiO_5 .

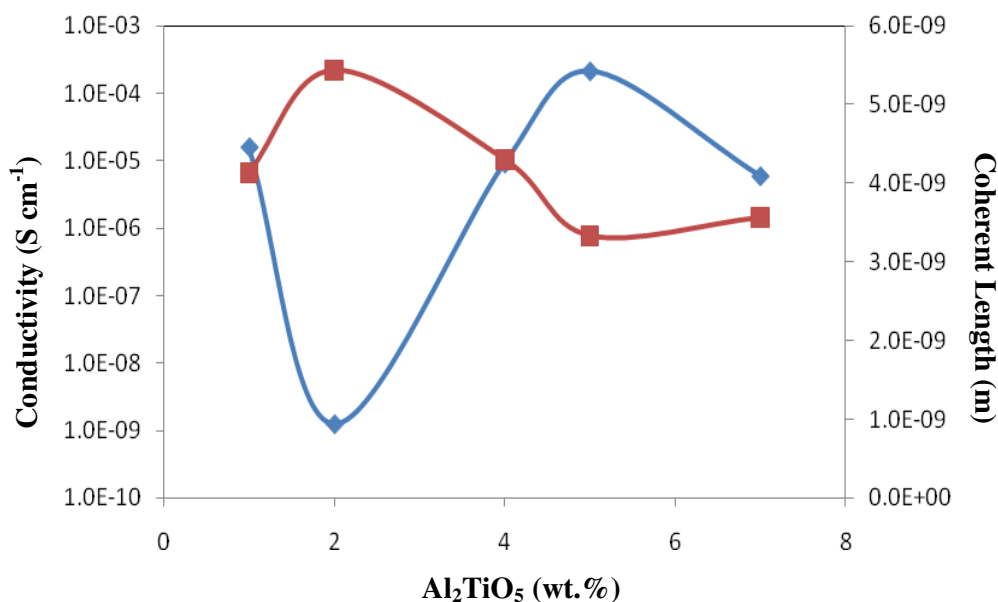


Fig. 7.6: Conductivity and coherent length again various Al_2TiO_5 (in wt. %)

7.6 Summary

The morphology of composite polymer electrolyte has been studied using SEM at room temperature. The effect of adding salt and filler has brought changes to the surface of chitosan complexes. By addition of Al_2TiO_5 into chitosan- acetate, the surface roughness increased with various sizes of agglomerates. The same pattern goes to sample with chitosan- NH_4SCN sample. XRD shows that some parts of the sample maintained its amorphousness from the broadness of the peak and some parts have become more crystalline. The coherent length is inversely proportional to conductivity. As coherent length decreased, conductivity increased and vice versa. Results from this chapter sheds some light in support of conductivity variation with Al_2TiO_5 content.